Transactions of the SMiRT 27
Yokohama, Japan, March 3-8, 2024
Division V

INVESTIGATION OF MULTIPLE IMPACT-DAMAGED REINFORCED CONCRETE STRUCTURES AS A REFERENCE FOR LIQUID PENETRATION BEHAVIOR AND TOMOGRAPHIC STUDIES

Marcus Hering[1], Georg Fiedler[2], Thomas Schubert[3], Falk Hille[4] Götz Hüsken[5] and Birgit Beckmann[6], Marcel Grunwald[7], Bernhard Redmer[8], Andreas Rogge[9]

[1]Dr.-Ing., Bundesanstalt für Materialforschung und –prüfung (BAM), Berlin, Germany (marcus.hering@bam.de)
[2]M.Sc., Bundesanstalt für Materialforschung und –prüfung (BAM), Berlin, Germany
[3]M.Sc. Technische Universität Dresden, Institut für Massivbau, Dresden, Germany
[4]Dr.-Ing., Bundesanstalt für Materialforschung und –prüfung (BAM), Berlin, Germany
[5]Dr. Dipl.-Ing., Bundesanstalt für Materialforschung und –prüfung (BAM), Berlin, Germany
[6]Dr.-Ing., Technische Universität Dresden, Institut für Massivbau, Dresden, Germany
[7]Bundesanstalt für Materialforschung und –prüfung (BAM), Berlin, Germany
[8]Dipl.-Ing., Bundesanstalt für Materialforschung und –prüfung (BAM), Berlin, Germany
[9]Dr.-Ing., Bundesanstalt für Materialforschung und –prüfung (BAM), Berlin, Germany

ABSTRACT

The structural integrity of outer reinforced concrete (RC) containments of nuclear power plants provides an essential shield against external hazards. If this containment is damaged by an impact event, such as an aircraft crash, the question arises to which degree the reinforced concrete containment still has its protective capability. This concerns both purely structural protection and protection against liquids penetrating the interior of the containment. Due to the dimensions of the containment structures, it is difficult to perform real scale impact experiments, so in the past decades plate geometries at medium scale have been used for investigations. Detailed investigations on the structural behaviour of RC members or RC plates subjected to impact loading have already been presented in Just et al. [1], Hering [2], Hering et al. [3-5], Bracklow et al. [6; 7], Hille et al. [8] and Nerger et al. [9].

The following investigations deal with the single and multiple impact event (first hard impact and/or subsequent soft impact) on a RC specimen, which provides the basis for further investigations. A description of the test setup and the test procedure as well as a presentation of the test results from the impact tests are provided.

Furthermore, the experimental program is presented, which the damaged RC specimens are to undergo to deal with the question of how much the impact-damaged RC structure has become permeable to liquid media, such as water and kerosene, depending on the intensity of the impact. The aim of these following investigations is to develop a test setup that can be applied to investigate the liquid penetration behaviour (LPB) of small, medium, and large-scale RC members.

In addition to the liquid penetration experiments, the damaged specimens are to be examined by planar tomography to obtain the damage inside the specimen. The combination of damaging event, fluid penetration behaviour and tomography should enable a comprehensive understanding of the damage to the RC specimen.

INTRODUCTION

Reinforced concrete (RC) has been used for many decades for protective structures that are designed to pwithstand dynamic impact loads. The complex physical properties of structural RC members lead to a difficult characterization under impact loading. However, it is not only the material properties that make characterisation so complex; the impact load and the description thereof also contribute to this. Directly related with this, the question arises to what level a structure is damaged as a result of an impact event and what the structural integrity of the RC structure is like. These influences are being systematically investigated as part of the multi-stage research project *Bauteilverhalten unter stoßartiger Beanspruchung durch aufprallende Behälter (Flugzeugtanks)* English: *Behaviour of structural components during impact load conditions caused by tank collisions (aircraft fuel tanks)*.

Previous investigations have shown that structures subjected to an impact load always exhibit a combination of global and local load-bearing behaviour. As a result, there is also a global and a localised damage behaviour, see [1-9]. The focus of the current investigations is on the local behaviour and the localised damage to the RC. An investigation of the combined global and local component behaviour or the component damage as a result of an impact event will be carried out as a follow-up to the investigations presented in this article.

The damage behaviour of RC structures is influenced by many factors like velocity, mass and shape of the projectile or dimension, strength and reinforcement configuration on the resistance side [10]. Furthermore, the type of impact also has a significant influence on component damage. A distinction is made between a soft and a hard impact. The hard impact is characterized by the fact that the impact object (the impactor) remains undeformed, whereby the affected structure is damaged. In the case of a soft impact, the impactor is deformed and the structure is not damaged, or at least less damaged [11-13]. However, the problem of whether it is a soft or hard impact can only be clearly separated in the laboratory. In reality, this load generally always occurs as a combination, see Sugano et al. [14-16]. For this reason, the localized damage of a hard and combined hard-soft impact will be presented.

In the following, the experimental programme and the tests already carried out will be described to provide an integral view of the material behaviour, the impact event, the damage and the resulting component permeability in order to establish a causal relationship. Furthermore, it is described which tests are still being carried out with the test specimens in order to obtain an integral understanding of the damage caused by the impact and the fluid permeability.

EXPERIMENTAL PARAMETERS AND TEST SETUP

RC Specimen

As previously described, localised damage as a result of an impact event should be the focus of the current experimental programme. For this reason, a cuboid specimen with edge lengths of 490 mm × 490 mm × 300 mm was selected. A similar approach was taken in Leicht [17].

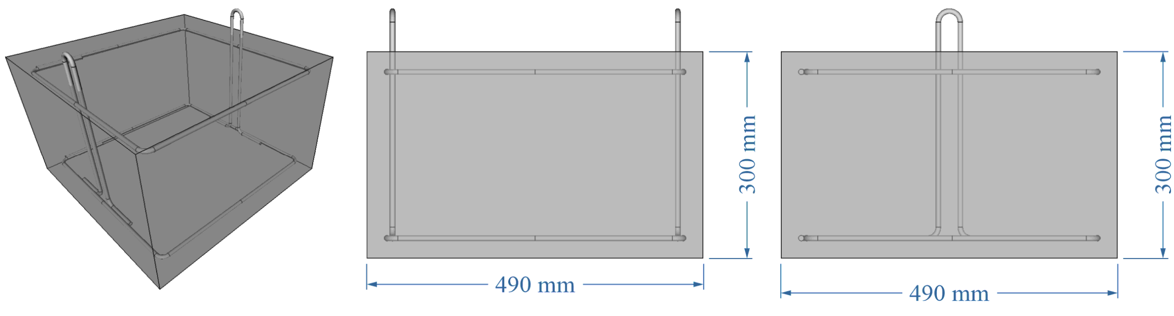

Figure 1. Geometry of the RC specimen.

In order to minimise the effect of the reinforcement as much as possible, only a circumferential ring was installed on the top and bottom of the specimen. In addition, two hangers were applied, which serve to transport the test specimen. The reinforcing steel (B500 B) used had a diameter of 8 mm and was laid with a concrete cover of 25 mm. An illustration of the test specimen can be found in Figure 1.

The concrete used is a C35/45 with a maximum grain size of 8 mm. It was poured in moulds with the geometry corresponding to the test specimen. After filling and compacting the concrete, it was covered with a PE foil to prevent it from drying out and to ensure good curing. The test specimens were demoulded on the 7th day. The test specimens were then stored under outdoor conditions in the yard of the Otto Mohr Laboratory (OML) of Technische Universität Dresden (TUD).

Experimental setup

The tests were carried out in the drop tower facility of the OML of the TUD. The accelerated configuration of the facility was used for the tests. The drop tower facility and the many technical details are described in Just et al. [1], Hering et al.[3-5] , Bracklow et al. [6; 7]. The impactor is accelerated through an approx. 11 m long acceleration pipe onto the RC target using pressurized air. The charge pressure controls the impact velocity of the impactor and thus makes it possible to achieve a high return accuracy for the test velocities.

The RC test specimen is placed on the top surface of four load cells (LC). To compensate for any unevenness on the surface of the test specimen, a mortar joint was provided between the load cell and the test specimen. The mortar used is an extremely fast hardening levelling mortar. The test setup consisting of LC's and RC specimen is shown in Figure 2 in both real and schematic form.

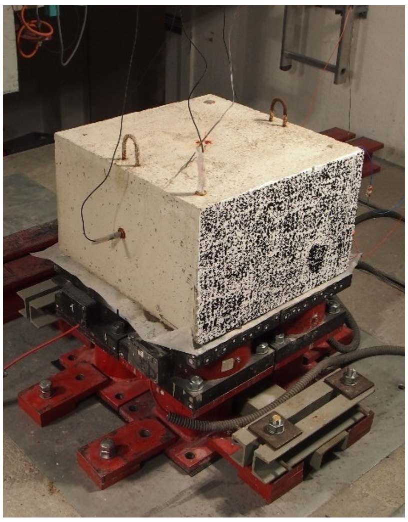

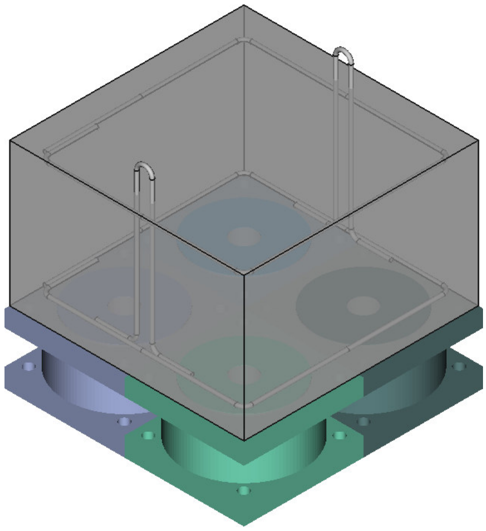

Figure 2. Test setup of RC test specimen on LC's and hard and soft impactors of 8.6 kg respectively

Different impactors were used to investigate the influence of the impact event on the damage to the test specimen. For the hard impact event, a flat steel cylinder with a diameter of 100 mm and a length of 160 mm was used. The impactor does not undergo any plastic deformation as a result of the impact with the RC block and can therefore be considered as rigid.

The deformable impactor consists of two parts. One is the 3 mm thick steel tube, which forms the deformable part of the impactor. The second is the additional mass attached to the rear end of the impactor, which can be used to control the impact energy by varying the total impactor mass. The outside diameter of the deformable part of the impactor is 95 mm. The impactor masses used in the test program are summarized in Table 1.

Measurement devices

The main measuring equipment used for the experimental investigations presented in this article are the four LC's on which the RC test specimen is placed. Each of these LC's has a maximum load capacity of 10,000 kN. In addition to the load cells, four acceleration sensors with a measuring range of 5,000 g were applied to the test specimen. Three of these measured the acceleration in the horizontal direction (perpendicular to the impact direction) and one accelerometer measured the acceleration of the RC specimen parallel to the impact direction. To measure the vertical Movement and velocity of the specimen after impact a laser Doppler vibrometer (LDV) was used which consist of the LDV and a reflector applied to a corner of the specimen. The measurement frequency of all sensors was 200 kHz.

The events during the experiment were also recorded with two high-speed cameras. The available image size is 1,024 px × 1,024 px at a frame rate of 7,000 fps. The pattern on the front side of the RC specimen also enables digital image correlation (DIC) of the experiment. However, this will not be part in this article.

EXPERIMENTAL PROGRAM

To investigate the localized damage to the reinforced concrete, single hard impacts were tested before measuring the result of a combined impact (first hard, then soft). Only the mass of the soft impactor was varied, not that of the hard impactor. The velocity was kept constant at approximately 50.0 m/s to simulate a single combined impact event. The choice of an impact velocity of 50.0 m/s is justified by the fact that this impact velocity, in combination with the 8.6 kg hard impactor, causes a moderate degree of damage to the test specimen. Higher impact velocities and/or mass would have resulted in excessive damage to the specimen, making the second impact test unnecessary. At lower velocities, there is too little damage caused by the hard impact. A systematic investigation of specimens that were only slightly damaged by the first impact and then had to withstand a soft impact was not carried out as part of this article. Preliminary tests have shown that only soft impactors do not cause cracks in the specimen.

The designation of the specimen, the type of impact and the mass of the impactor are given in Table 1. The average impact velocity measured during the tests was 50.7 m/s. Q13 is the reference for the hard impact. Subsequently, specimens that had previously been struck by the same hard impact were additionally damaged by a soft impact of different weights (specimens Q10 to Q12). Before the second impact, the specimens were repositioned to hit the same spot as the previous hard impact. For all 7 impacts, the measured support forces and damage on all sides were documented.

Table 1: Experimental program.

Specimen label	Type of impact	$v_{\text{imp,hard}}$ [m/s]	$m_{\text{imp,hard}}$ [kg]	$v_{\text{imp,soft}}$ [m/s]	$m_{\text{imp,soft}}$ [kg]
Q13	hard	50.5	8.6	/	/
Q12	hard/soft	50.0	8.6	50.5	8.6
Q11	hard/soft	51.3	8.6	50.9	11.3
Q10	hard/soft	51.2	8.6	50.8	14.0

RESULTS

The hard impacts with the same mass led to similar damage results in terms of crack pattern. Figure 3 shows an example of a crack pattern for both hard and soft impact. The hard impactor penetrated the specimen to about 1-2 mm. Only very small amounts of scabbing at point of impact had been recorded.

The crack width for the already cracked specimens was substantially larger after the additional soft impacts. More precise information on the crack widths will be collected when the results of the planar tomography are available. In general, the damage and penetration depth increased as the mass of the soft impactor increased.

Figure 3. Damage results for a hard (left) and hard then soft (middle) and soft impactor Q11 after impact (right).

The support forces of the four LC's were aligned to the time of contact on top of the specimen ($t = 0$ ms). Because the LC's measured similar forces, the forces were added up. In Figure 4 the sum of the support forces is displayed for hard and soft impact. In the case of a hard impact, the measured support forces increase slightly according to the increasing speed. The two maxima in sequence were characteristic of the experiments carried out. However, for hard impacts the first maxima was always the larger of the two. Both maxima of the support forces are documented in Table 2. Although the speeds only vary slightly, the maximum support forces range from 1,300 to 2,200 kN.

The maximum support forces for a soft impact are significantly lower at only one fourth of the hard impact. At higher impactor masses and consequently higher loads, there is a clear plastic deformation of the impactor. It folds up on the side that has been hit (see Figure 3). Due to the higher mass and thus higher kinetic energy, the force-time curves differ in their duration. The force duration is also documented in Table 2. Counterintuitive the measured maximum force of the heaviest impactor Q10_soft is the lowest, although only slightly. However, comparing the momentum i.e., the area under each graph for the time of loading it becomes apparent, that a heavier impactor leads to bigger momentum.

The measurement of the horizontal acceleration shows the movement away from the impact point and thus the intensity of deformation of the crack edges. The accelerations in Table 2 vary greatly, as the development of cracks is subject to strong fluctuations in the tensile load-bearing capacity. A correlation between measured acceleration and determined degree of destruction cannot be clearly characterized.

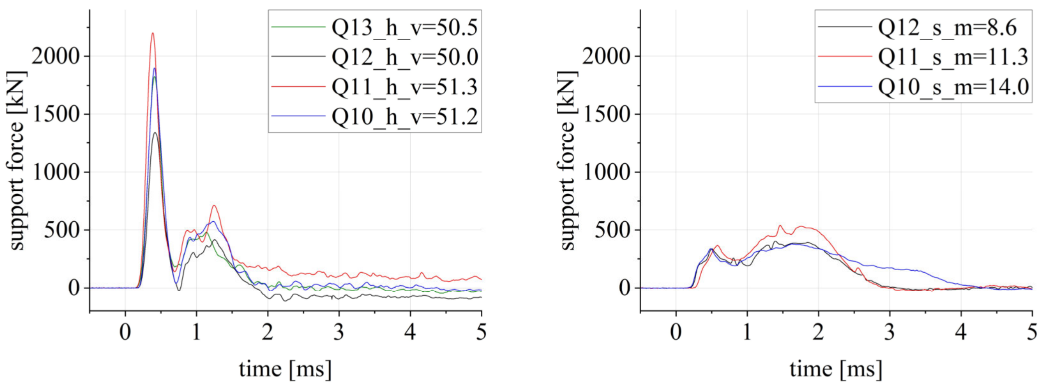

Figure 4. Sum of the support forces over time for hard (left) and soft (right) impact.

Table 2: Measured forces and acceleration of impact loading.

	Specimen label	F_{max} [kN] First peak	F_{max} [kN] Second peak	$t_{load,approx.}$ [ms]	p [Ns]	$a_{h,max}$ [m/s²]	$a_{v,max}$ [m/s²]
hard	Q13_h_v=50.5	1,826.9	479.1	1.9	731.2	60307	72,867
	Q12_h_v=50.0	1,341.6	416.4	2.2	534.6	122,377	104,850
	Q11_h_v=51.2	2,203.6	711.5	1.9	939.6	63,050	147,249
	Q10_h_v=51.3	1,899.8	573.4	1.8	794.3	155,316	153,997
soft	Q12_s_m=8.6	329.8	401.2	2.8	672.1	39,947	118,929
	Q11_s_m=11.0	363.6	540.8	2.8	822.8	20,566	34,756
	Q10_s_m=14.0	333.8	375.9	4.0	862.2	25,570	44,849

As the cuboid was not attached to the LC's, it lifts upwards due to the rebound from the LC's. This corresponds to the residual energy of the specimen after impact. In Figure 5, measured by the LDV the vertical movement of the specimen is shown. The velocity graphs of the hard impact are smoothed over 500 data points, those of the soft impact over 5,000 points. A moving average with 500 data points at a measuring rate of 200 kHz corresponds approximately to a 200 Hz low-pass filter and a moving average with 5,000 data points at the same measuring rate corresponds approximately to a low-pass filter of 20 Hz. During the time in which no force is measured, the test specimen is in the air (airtime). Especially for the hard impact, the parabolic course of the travelled distance and linearly varying velocities for the upper side over time is clearly visible. Since no further forces on the specimen act after rebound the linear change in velocity corresponds to the gravitational acceleration g. The reflector of the LDV for the hard impact Q12 came loose, therefore the actual deflection of this specimen, as printed in Figure 5, cannot be regarded as comparable. The initial velocity during take-off cannot be determined due to the large noise. However, in case of a vertical upward momentum, the minimal velocity before touchdown also corresponds to the initial velocity if only gravitational force applies. The minimal velocities are summarized in Table 3 Since no vertical deflection can be determined for Q12, all distances were calculated with the initial velocity.

With the soft impact, a similar picture can only be approximated since the specimens were already partially destroyed. The airtime and thus initial velocity appear to be greater. Because of the large noise, velocity values were calculated over airtime in Table 3. It can be assumed that the specimen behaved less rigid due to the destruction, which is why the measured velocities varies greatly. A correlation between impact velocity and lift-off velocity for the hard impact is visible in Table 3. No correlation can be seen for the soft impact.

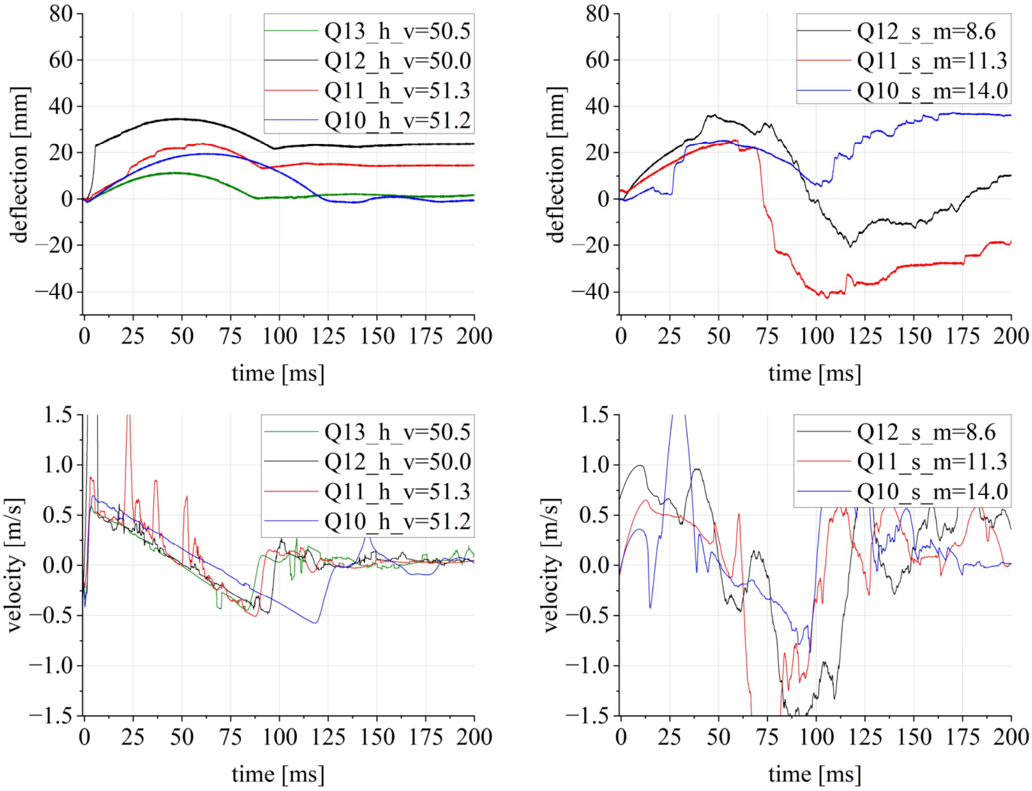

Figure 5. Deflection and velocity over time for hard (left) and soft (right) after impact.

Table 3 measured airtime and velocity with calculated maximum vertical deflection after impact.

	Specimen label	$t_{c,air}$ [ms]	v_c [m/s]	$s_{c,vert.,calc.}$ [mm]
hard	Q13_h_v=50.5	86.5	0.45	11.6
	Q12_h_v=50.0	95.4	0.48	11.7
	Q11_h_v=51.2	89.3	0.50	13.1
	Q10_h_v=51.3	124.3	0.57	16.7
soft	Q12_s_m=8.6	115.4	0.57	16.3
	Q11_s_m=11.0	99.8	0.49	12.2
	Q10_s_m=14.0	99.9	0.49	12.2

CONCLUSION

The tests were selected in such a way that just small/intermediate cracks were caused to the test specimens in the event of a hard impact. The experimental series showed that the damage could be significantly increased by the combined impact event (hard impact followed by soft impact). Significant differences were found in the measured support forces. For the soft impact the maximum force is only one fourth of the hard impact, but with similar momentum. After the moderate documented damage from the hard impact the soft impact increased the spalling/scabbing substantial (see Figure 3). Therefore, already formed cracks and microstructural defects in the specimen influence the degree of damage significantly.

With the measured velocities for the specimen and impactor after impact the converted delta of kinetic energy can be calculated. The next step is to compare the results with the internal damage using tomography and the energy losses after impact using photogrammetry.

OUTLOOK AND FURTHE INVESTIGATIONS

Liquid penetration behaviour

The investigations presented so far in this article simply form the basis for further considerations. In addition to the tomographic investigations described in the following section, another way of characterising the damage is considered. This is the leakage resistance of the damaged RC structure. In addition to the tomographic images, examination of the liquid penetration behaviour provides an indication of the integrity of the damaged structure. Where tomography is difficult to evaluate due to image resolution, the penetration behaviour can still provide integral conclusions about the internal crack structure.

Figure 6 shows the test rig developed at BAM to determine the liquid penetration behaviour. The test pressure can be adjusted up to 2.5 bar by means of the installed fittings. The current maximum flow rate is 25 litres/min. At the same time, the fluid pressure in the system under test is measured at two points. This is complemented by continuous measurement of the fluid flow rate. Longitudinally split cylindrical specimens are currently being examined to characterise the penetration behaviour through a discrete crack. A study on leakage resistance for impact-damaged RC cuboids is also planned, once the tomographic studies have been completed.

Figure 6. Experimental set-up for determination of liquid penetration behaviour.

Planar Tomography

Once specimens with clearly defined damage have been produced by impact events, they will be further examined. Firstly, the RC samples are to be X-rayed using planar tomography. The High Energy X-ray Laboratory (HEXY-Lab) at BAM will be used for this purpose. The special feature of this facility is that the radiation source, the examined object and the detector can be moved in 13 axes (9 linear and 4 rotational axes). The maximum possible geometry to be scanned is 4 m in length and 1.5 m in height and the maximum weight is 2 t. The radiation source is a betatron that can accelerate a voltage of 7.5 MeV. Thus, thicknesses of up to 30 cm can be scanned. The detector used is a high-resolution matrix detector (XRD1620) as DDA (Digital detector array) from PerkinElmer, see Figure 7.

With the help of radiographic investigations, the crack patterns inside the RC samples are to be examined in more detail. The main focus here is on the resulting cracks with the associated crack widths and the resulting crack volumes. Furthermore, the extent to which the damage is increased by the second impact event is to be investigated.

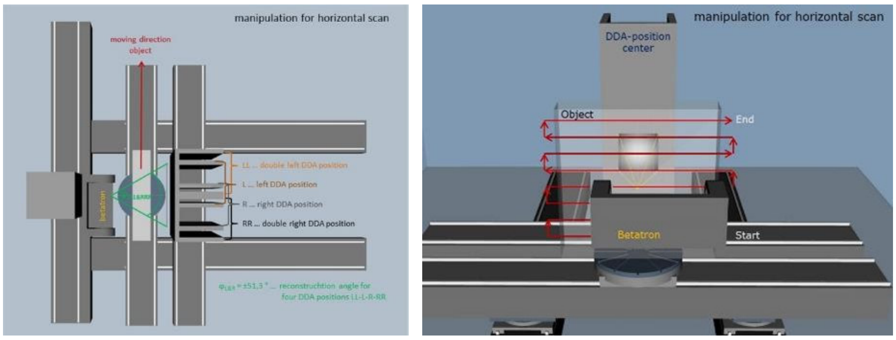

Figure 7. Schematic illustration of the HEXY-Lab, see Nerger et al. [9].

Description of Figure 7: Scanned planar tomography - horizontal arrangement. Emitter and detector are moved synchronously and in parallel along the red line and several hundred individual projections are recorded. Left: Illustration of the horizontal detector positions LL – L – R - RR. Right: Horizontal travel over several "contour lines" for scanning the entire test object surface

The data resulting from the x-ray consists of voxels with side lengths of 0.5 mm in the plate plane and 1.5mm in the depth direction. Smaller details cannot be recorded with this method.

During reconstruction, an overall 3D image is assembled from the filtered 2D projections on the reverse side. The grey values created by different exposures result in the contrast required for the reconstruction. With higher contrast, inhomogeneities such as cracks, pores or reinforcement can be found more easily.

The deep learning program *Dragonfly* is used, which was previously taught "special features" such as cracks, etc. in a labelling process. With sufficient experience *Dragonfly* recognizes and labels voxels on its own, which can be used for further analysis.

ACKNOWLEDGMENTS

The presented projects were funded by the German Federal Ministry for the Environment, Nature Conservation, Nuclear Safety and Consumer Protection (BMUV) under the grant numbers 1501541, 1501542, 1501647 and 1501648 on basis of a decision by the German Bundestag.

Special thanks go to the staff of the Otto Mohr Laboratory. Without their active support and technical expertise, it would not have been possible to carry out such a comprehensive test program.

Gefördert durch:

Bundesministerium
für Umwelt, Naturschutz, nukleare Sicherheit
und Verbraucherschutz

aufgrund eines Beschlusses
des Deutschen Bundestages

REFERENCES

[1] Just, M., Curbach, M., Kühn, T., & Hering, M. (2016). *Bauteilverhalten unter stoßartiger Beanspruchung durch aufprallende Behälter (Flugzeugtanks); Phase 1A: Maßstabseffekte bei stoßartiger Beanspruchung. Reaktorsicherheitsforschungs-Vorhaben Nr. 1501438.*

[2] Hering, M. (2020). *Untersuchung von mineralisch gebundenen Verstärkungsschichten für Stahlbetonplatten gegen Impaktbeanspruchungen* [Dissertation, Technischen Universität Dresden]. Dresden. https://nbn-resolving.org/urn:nbn:de:bsz:14-qucosa2-737908

[3] Hering, M., Kühn, T., & Curbach, M. (2017). *Bauteilverhalten unter stoßartiger Beanspruchung durch aufprallende Behälter (Flugzeugtanks); Phase 1B: Quantifizierung der Schädigungen des Betongefüges, Teilprojekt: Fallturmversuche. Reaktorsicherheitsforschungs-Vorhaben Nr. 1501479.*

[4] Hering, M., Bracklow, F., Kühn, T., & Curbach, M. (2019). Impact experiments with reinforced concrete plates of different thicknesses. *Structural Concrete*, *21*(2), 587-598. https://doi.org/10.1002/suco.201900195

[5] Hering, M., Bracklow, F., & Curbach, M. (2022, 10.-15. July 2022). *Impact Experiments on Scaled Reinforced Concrete Plates* 26th International Conference on Structural Mechanics in Reactor Technology (SMiRT 26), Berlin/Potsdam, Germany.

[6] Bracklow, F., Hering, M., Beckmann, B., & Curbach, M. (2021). *Bauteilverhalten unter stoßartiger Beanspruchung durch aufprallende Behälter (Flugzeugtanks); Phase 1C: Experimentelle und numerische Untersuchungen zu Maßstabseffekten, Versagensmechanismen und Bauteilschädigung. Reaktorsicherheitsforschungs-Vorhaben Nr. 1501541.*

[7] Bracklow, F., Hering, M., Beckmann, B., & Curbach, M. (2022, 10.-15. July 2022). *Impact Experiments on Differently Reinforced Concrete Plates* 26th International Conference on Structural Mechanics in Reactor Technology (SMiRT 26), Berlin/Potsdam, Germany.

[8] Hille, F., Rogge, A., Nery, G., & Redmer, B. (2017). *Bauteilverhalten unter stoßartiger Beanspruchung durch aufprallende Behälter (Flugzeugtanks); Phase 1B: Quantifizierung der Schädigungen des Betongefüges. Reaktorsicherheitsforschungs-Vorhaben Nr. 1501477.*

[9] Nerger, D., Moosavi, R., Grunwald, M., Hille, F., Redmer, B., & Rogge, A. (2020). *Bauteilverhalten unter stoßartiger Beanspruchung durch aufprallende Behälter (Flugzeugtanks); Phase 1C: Weiterführende Untersuchungen zur Quantifizierung der Schädigungen des Betongefüge. Reaktorsicherheitsforschungs-Vorhaben Nr. 1501542.*

[10] Li, Q. M., Wen, H. M., & Telford, A. R. (2005). Local impact effects of hard missiles on concrete targets. *International Journal of Impact Engineering*, *32*(1-4), 224-284. https://doi.org/10.1016/j.ijimpeng.2005.04.005

[11] Vepsä, A., Saarenheimo, A., Tarallo, F., Rambach, J.-M., & Orbovic, N. (2011, 6.-11. November 2011). *IRIS_2010 PART II: Experimental Data* 21st International Conference on Structural Mechanics in Reactor Technology (SMiRT 21), New Delhi, India.

[12] Saarenheimo, A., Tuomala, M., Calonius, K., Vepsä, A., & Hakola, I. (2013, 18.-23. August 2013). *Bending and shear punching studies on impact loaded reinforced concrete wall, Part 1* 22nd International Conference on Structural Mechanics in Reactor Technology (SMiRT 22), San Francisco, California, USA.

[13] Saarenheimo, A., Calonius, K., & Tuomala, M. (2015, 10.-14. August 2015). *Bending and punching studies on impact loaded plate* 23th International Conference on Structural Mechanics in Reactor Technology (SMiRT 23), Manchester, United Kingdom.

[14] Sugano, T., Tsubota, H., Kasai, Y., Koshika, N., Orui, S., von Riesemann, W. A., Bickel, D. C., & Parks, M. B. (1993). Full-scale aircraft impact test for evaluation of impact force. *Nuclear Engineering and Design*, *140*, 373-385.

[15] Sugano, T., Tsubota, H., Kasai, Y., Koshika, N., Ohnuma, H., von Riesemann, W. A., Bickel, D. C., & Parks, M. B. (1993). Local damage to reinforced concrete structures caused by impact of aircraft engine missiles Part 1. Test program, method and results. *Nuclear Engineering and Design*, *140*, 387-405.

[16] Sugano, T., Tsubota, H., Kasai, Y., Koshika, N., Itho, C., Shirai, K., von Riesemann, W. A., Bickel, D. C., & Parks, M. B. (1993). Local damage to reinforced concrete structures caused by impact of aircraft engine missiles Part 2. Evaluation of test results. *Nuclear Engineering and Design*, *140*(407-423).

[17] Leicht, L. (2022, 26.-27. September 2022). *Charakterisierung von mineralisch gebundenen Kompositen zur Impaktdämpfung* 61. Forschungskolloquium mit 9. Jahrestagung des DAfStb, Dresden, Germany.